12^{th} International Conference on Fracture Mechanics of Concrete and Concrete Structures
FraMCoS-12
B.L.A. Pichler, Ch. Hellmich, P. Preinstorfer (Eds)

https://doi.org/10.21012/FC12.1116
MS06-1:1

LINEARITY AND ASSESSMENT OF MICRO-SCALE CREEP IN C-S-H VIA NANOINDENTATION

JIŘÍ NĚMEČEK, JITKA NĚMEČKOVÁ AND JIŘÍ NĚMEČEK*

* Czech Technical University in Prague, Faculty of Civil Engineering, Department of Mechanics
Thákurova 7, 166 29, Prague 6, Czech Republic
e-mail: jiri.nemecek@fsv.cvut.cz

Key words: Nanoindentation, Cement paste, Creep compliance, Calcium-Silicate-Hydrate

Abstract. This paper focuses on quantifying the micro-scale creep compliance of the C-S-H phase in well-hydrated, 1.5-year-old cement paste, measured using grid nanoindentation with a Berkovich tip. Four different load levels were tested to induce varying levels of deformation and stress. The results showed that the measured creep compliance is independent of the maximum vertical force within the range of 1 mN to 3 mN, standardly used in nanoindentation of cement pastes. The same trends and conclusions were observed for a reference polymeric material, PMMA, chosen for its homogeneity. In both cases, the creep falls in the linear viscoelastic regime. The linearity was further checked by calculation of the stress developed beneath the indentation tip. The stress was estimated using a finite element numerical model simulating the contact problem. The calculated stress reached 61.4% of the compressive strength measured by micro-pillar testing, 17.1%–46.1% of the strength measured by micro-beam testing, and 29.0% of the strenght estimated by the multiscale model.

1 INTRODUCTION

Long-term creep deformations in bridges and other structures subjected to permanent loads are well-known, typically following a logarithmic or power-law behavior over extended time scales [1]. Nowadays, analogous creep deformations can be measured at the micro-scale for individual hydrated cement phases using a nanoindenter [2, 3]. The main hydration product, calcium silicate hydrate (C-S-H), exhibits similar creep behavior [4, 5], though on a very different time scale compared to structures [1]. Given that the indenter induces high stresses under the tip [6], exceeding largely the macroscopic uniaxial strength of concrete, the question arises as to whether the micro-scale creep observed in nanoindentation remains in the linear regime [7] and allowing for classical linear viscoelastic models or upscaling of linear viscoelastic properties [8] to be used. Thus, this study aims to determine whether the creep compliance of cement pastes (or more specifically C-S-H gels), assessed by nanoindentation at the micro-scale, is measured in the linear regime. The task was solved through the application of various nanoindentation loading protocols with progressively increasing maximum force intensities, as well as through stress analysis beneath the indenter tip using numerical modeling.

2 EXPERIMENT AND METHODS

2.1 Materials and samples

Two types of samples were used for nanoindentation creep measurements. The first sample type was an ordinary cement paste prepared from Portland cement (CEM I 42.5R produced by Holcim, Czech Republic) with the water-to-cement ratio of 0.4. The second material type was a poly-methyl-methacrylate glass (PMMA, PLEXIGLAS® GS produced by Evonik Röhm

GmbH, Germany), chosen as a reference due to its single-phase structure with homogeneous properties in a wide range of scales. Cement paste samples were cast in cylindrical molds (28 mm in diameter and 70 mm in height), cured in the molds for 24 hours, then demolded and submerged in a 1% limewater solution for 1.5 years. After curing, the samples were cut into 6 mm thick slices using a precision diamond-blade saw. The slices were then polished with silicon carbide papers of grit sizes #2000 and #4000 to ensure consistent removal of loose particles resulting in surface root mean-square (RMS) roughness 41.2±9.8 nm. Details of the polishing procedure are provided in [9]. A prismatic PMMA sample (35×35×4 mm^3) was used without further polishing, as its surface was already smooth after the casting process of sample fabrication.

2.2 Nanoindentation setup

Nanoindentation was performed using a Hysitron TI–980 (Bruker, USA) equipped with a Berkovich diamond tip. A trapezoidal load function was applied, consisting of a 0.1 s linear loading phase up to the maximum force, followed by a 40 s holding period and a 1 s linear unloading. A very short linear loading time was chosen to simulate a step loading and to minimize creep deformation otherwise appearing during the loading phase. Also, a relatively short holding period was selected to reduce thermal drift deformation during creep measurements. The parameters were found as optimal for creep testing based on our previous research [10].

The maximum forces, usually used in nanoindentation of cement pastes, were set at four levels (1000 µN, 1500 µN, 2000 µN, and 3000 µN). Five levels were chosen for PMMA (250 µN, 500 µN, 750 µN, 1000 µN, and 1500 µN). For cement paste, the lower force threshold was selected to ensure results were unaffected by surface roughness, while the upper threshold was chosen to measure C-S-H phases without phase interactions with Portlandite or unhydrated clinker that could be caused by higher forces. For PMMA, the maximum forces were selected to achieve similar contact depths to those measured in cement paste samples.

To obtain a large statistical dataset at each maximum force, a grid of 22 × 18 indents (396 indents) was prescribed for cement paste, with individual indents separated by 10 µm. Due to the homogeneity of the sample, a smaller grid of 7 × 7 indents (49 indents) with the same separation was used for PMMA.

2.3 Methodology

The elastic behavior of the material can be determined from the unloading portion of the load-displacement curve using the Oliver and Pharr theory [11], and the indentation (reduced) modulus is calculated as:

$$E_r = \frac{S\sqrt{\pi}}{2\beta\sqrt{A_c}}, \tag{1}$$

where A_c is the projected contact area dependent on contact depth h_c, S is the contact stiffness, and β is the geometry correction factor assumed to be 1.034 for a Berkovich tip.

A relationship between the time-dependent indentation load, $P(t)$, and displacement, $h(t)$, for a viscoelastic solid considering a step-up loading scenario, along with a correction for all inelastic (predominantly plastic) deformations created by a sharp (Berkovich) tip, can be formulated as [5]:

$$(h(t) - h_0)^2 = \frac{\pi}{2\tan\alpha} P_{max} J(t), \tag{2}$$

where P_{max} is the maximum force, α is the cone-equivalent angle (assumed to be 70.3° for the Berkovich tip), h_0 is the correction factor accounting for the amount of inelastic deformation occurring during the loading phase, and $J(t)$ is the creep compliance function. Assuming the Kelvin chain model [3, 12], $J(t)$ can be approximated as:

$$J(t) = \frac{1}{E_r} + \sum_{i=1}^{N} \frac{1}{E_i} \left(1 - e^{-\frac{t}{\tau_i}}\right) RCF_i \tag{3}$$

where E_i and τ_i are the elastic moduli and retardation times of the Kelvin units, respectively,

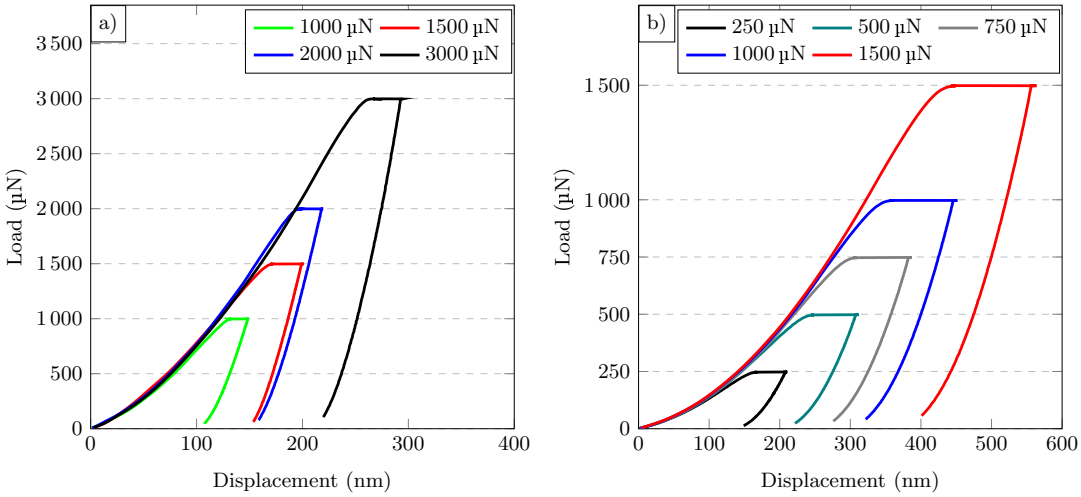

Figure 1: Typical load-displacement curves measured on (a) cement paste and (b) PMMA.

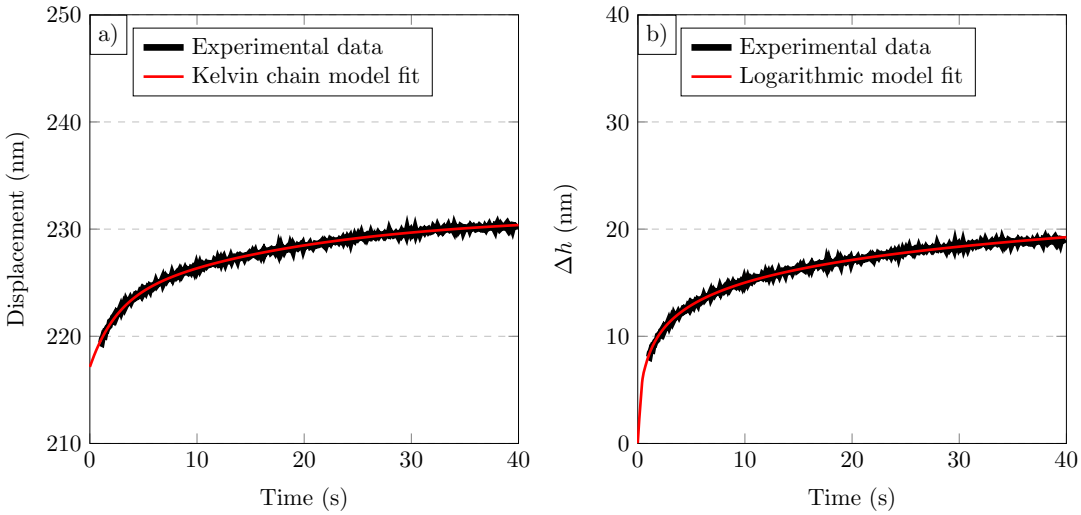

Figure 2: Example of fitting experimental data measured for cement paste under a maximum force of 2000 µN with (a) Kelvin chain model using Eqs. 2 and 3 and (b) with the logarithmic model, Eq. 4.

and RCF_i is the ramp correction factor that accounts for the non-zero duration of the loading period.

The occurrence of time-independent plasticity in the loading phase can also by accounted for by the approach of Vandamme et al. [2, 4], who assumed the logarithmic function and the creep compliance function as follows:

$$J(t) - \frac{1}{E_r} = \frac{2a_c\Delta h(t)}{P_{max}} = \frac{ln(1+t/\tau)}{C} \quad (4)$$

where $\Delta h(t)$ is the increment of measured displacement during the holding period, a_c is the tip contact radius, C denotes the creep modulus, and τ represents the characteristic time.

3 RESULTS AND DISCUSSION

3.1 Results of cement paste

Initially, the reduced modulus was evaluated from the load-displacement curves. All the data were then merged, and the main C-S-H gel-based phase was separated using the statistical deconvolution method [13], resulting in an average C-S-H modulus of $E_r = 30.2 \pm 5.4$ GPa. Example of typical indentation curves with a mean E_r value is shown in Fig. 1a for all four maximum force variants.

The creep compliance was subsequently evaluated only for a narrow interval of reduced moduli in the range of 28–32 GPa to minimize

Table 1: Viscoelastic parameters derived from the Kelvin chain model and the logarithmic model, measured for C-S-H.

Kelvin chain model (Eqs. 2, 3)						Logarithmic m. (Eq. 4)	
P_{max}	E_1	τ_1	E_2	τ_2	h_0	C	τ
(μN)	(GPa)	(s)	(GPa)	(s)	(nm)	(GPa)	(s)
1000	517±122	2.1±0.5	308±94	16.7±5.3	18.0±10.1	505±75	0.15±0.06
1500	492±186	2.3±0.4	288±108	16.9±4.4	36.3±17.4	492±97	0.11±0.07
2000	517±111	2.3±0.5	355±96	16.3±4.7	39.7±9.8	477±96	0.05±0.03
3000	533±104	2.1±0.3	353±70	14.4±2.9	46.4±13.5	541±96	0.09±0.01

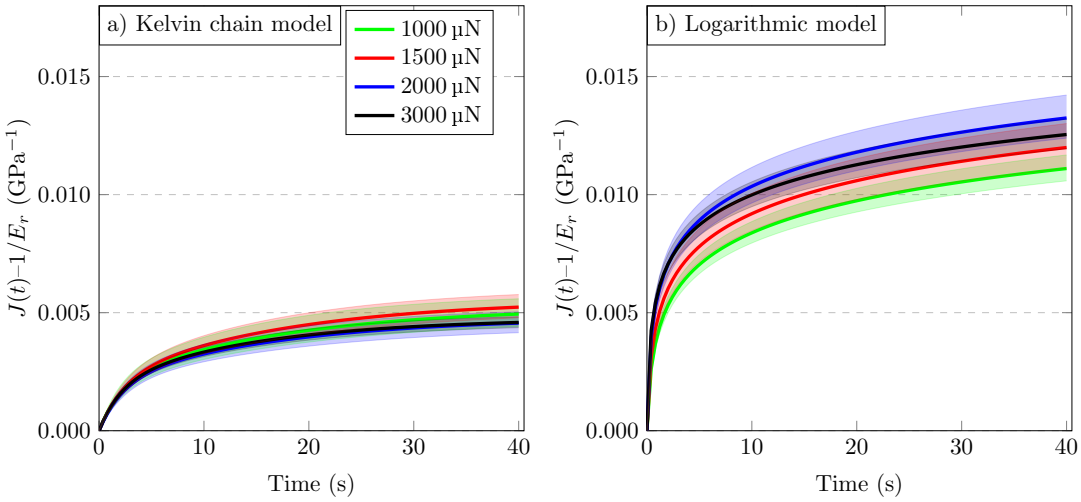

Figure 3: Creep compliance functions calculated for cement paste with (a) Kelvin chain model using Eqs. 2 and 3 and (b) with the logarithmic model, Eq. 4.

the overlapping with other phases. Additionally, all the data with thermal drift, measured by the nanoindenter, larger than 0.05 nm/s were excluded from the evaluation procedure, leaving a set of 35 (1000 μN), 75 (1500 μN), 48 (2000 μN), 73 (3000 μN) indents suitable for analyses. Both the Kelvin chain model with two units and the logarithmic model were used for evaluation. Due to the instrument instability in capturing the transition between loading and holding periods, caused by very short loading times (0.1 s), the holding period data were fitted in the range of 1–40 s. An example of the fitting procedure is shown in Fig. 2, demonstrating excellent fits for both models.

The creep compliance data, with the spread calculated as 95% confidence intervals, is shown in Fig. 3. It can be observed that the logarithmic model, compared to the Kelvin chain model, predicts significantly higher values for the $J(t)$ functions while maintaining the same general behavior. In both cases, the measured curves are closely aligned, with no apparent dependency on the maximum force. The differences are likely due to sample heterogeneity and, the low statistical sample size, which is given by the overlapping data spread.

The calculated model parameters, summarized in Table 1, exhibit an almost constant trend for E_1, E_2, τ_1, τ_2, and C though the large standard deviations in the measured constants highlight the sample heterogeneity. This consistency suggests measurements were performed within the linear regime. Other parameters, such as h_0 (Fig. 5), show a linear increase, whereas τ exhibits a linear decrease with increasing maximum force. These observations were similarly noted for a homogeneous reference PMMA sample, as discussed in the following Section 3.2.

Table 2: Viscoelastic parameters derived from the Kelvin chain model and the logarithmic model, measured for PMMA.

Kelvin chain model (Eqs. 2, 3)						Logarithmic model (Eq. 4)	
P_{max} (μN)	E_1 (GPa)	τ_1 (s)	E_2 (GPa)	τ_2 (s)	h_0 (nm)	C (GPa)	τ (s)
250	26.3±1.0	2.46±0.24	16.5±0.7	20.9±2.0	2.2±1.0	24.1±0.6	0.10±0.02
500	26.3±0.7	2.45±0.13	16.5±0.5	21.2±1.5	16.6±0.7	24.2±0.4	0.10±0.01
750	26.4±0.5	2.46±0.08	16.6±0.3	21.4±1.1	27.9±0.7	24.6±0.3	0.09±0.01
1000	26.8±0.4	2.42±0.08	16.6±0.8	21.4±0.8	38.4±0.9	24.8±0.3	0.09±0.01
1500	26.2±0.5	2.43±0.11	15.7±1.1	23.4±2.3	56.8±0.6	24.9±0.3	0.08±0.01

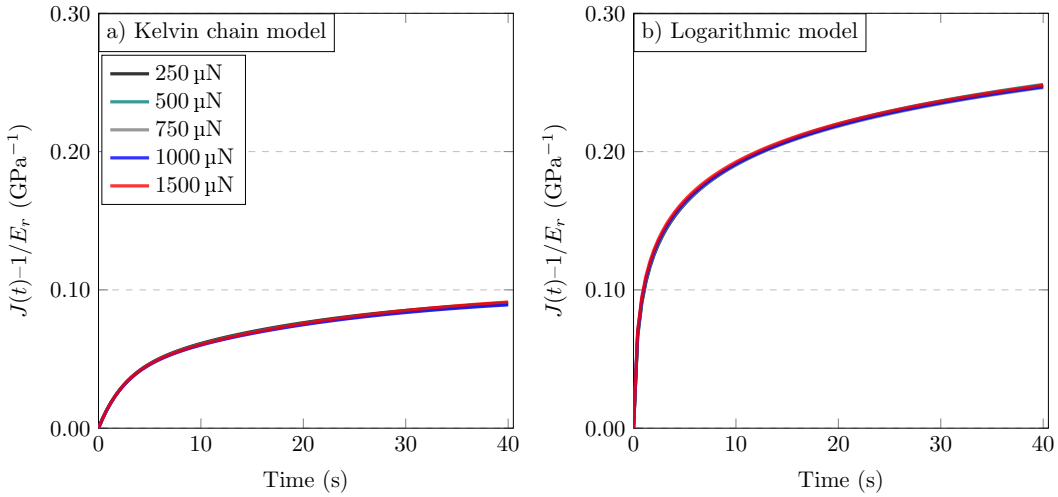

Figure 4: Creep compliance functions calculated for PMMA using (a) the Kelvin chain model and (b) the logarithmic model.

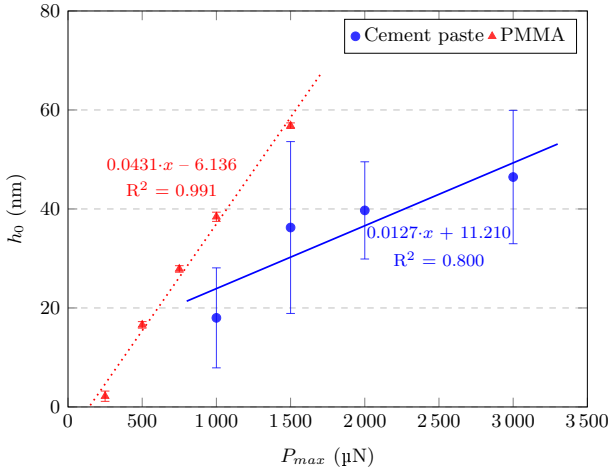

Figure 5: Evolution of h_0 parameter with increasing maximum load.

3.2 Results of PMMA

For the PMMA sample, the only indents excluded from the evaluation were those with a thermal drift exceeding 0.05 nm/s (Fig. 1b). The PMMA sample exhibited a creep behavior analogous to that observed in the cement paste. However, since the measurements were not influenced by sample heterogeneity, the $J(t)$ functions are nearly identical for all five maximum force intensities, even though the two models yielded different $J(t)$ magnitudes. An example of the creep compliance evaluated using both models is shown in Fig. 4. The minimal influence of the maximum force is also reflected in the calculated viscoelastic constants (see Table 2), which remain almost unchanged in all cases except for the parameters h_0 and τ. The parameter h_0 increases linearly with increasing P_{max} (Fig. 5), supporting the conclusion that the amount of accumulated plastic deformation scales linearly with the force and the creep compliance is measured within the linear regime.

3.3 Numerical simulation of the stress field under the nanoindenter tip

To support the above observation on the linearity of viscoelastic response in nanoindentation, the stress field under the tip was calculated and compared with the stress limits standardly checked on the macro-scale. For concrete samples, the linear regime is usually assumed if the stress is below 40–60% of their compressive strength [7]. Consequently, the actual stress beneath the tip was calculated using a finite element (FE) numerical model accounting for the real bluntness of the tip.

An axisymmetric contact problem involving a Berkovich tip with the substrate, reflecting the real tip geometry, was modeled in ANSYS software. The substrate domain was assumed to be $15 \times 15\,\mu m^2$ and was meshed with quadrilateral elements (PLANE182) of size $0.1\,\mu m$. The contact was modeled as frictionless using the CONTA172 and TARGE169 elements [14]. The tip material was assumed to be elastic and isotropic, with properties corresponding to diamond. The material of C–S–H was modeled using a visco-elasto-plastic model.

The elastic response was modeled using isotropic elasticity with Young's modulus of 30.2 GPa and a Poisson's ratio of 0.2. J2-plasticity was assumed with bilinear isotropic hardening, defined by a yield strength of 360 MPa and a tangent modulus of 1800 MPa. The viscous response was modeled using creep time hardening, where the change in equivalent creep strain with respect to time is defined by the following equation:

$$\dot{\varepsilon}_{cr} = C_1 \sigma^{C_2} t^{C_3} e^{-C_4/T}, \tag{5}$$

where σ is equivalent stress, T is the temperature, t is the time at end of substep and, C_1 through C_4 are the model constant ($C_1 = 1.25 \times 10^{-7}$, $C_2 = 1.195$, $C_3 = 0.11$, $C_4 = 0$). The visco-plastic constants were calibrated to ensure the simulated response matched the experimental load-displacement curve closely (Fig. 6). As an example, Fig. 7 shows the calculated Von Mises stress beneath the tip as 958 MPa (for load level of $3000\,\mu N$). Other load cases yielded stresses of 687 MPa ($1000\,\mu N$), 734 MPa ($1500\,\mu N$), 799 MPa ($2000\,\mu N$).

The compressive strength is, however, difficult to measure at the micro-scale. Němeček et al. found the tensile strength of micro-beams in C-S-H phases is 260–700 MPa [15]. Based on a simple Grifith-type model used in [16], the ratio of the uniaxial compressive-to-tensile strength equals 8, leading to an estimate of C-S-H compressive strength 2080–5600 MPa. The compressive strength of C–S–H measured directly by micro-pillar compression in a vacuum was reported as 1560±600 MPa [17]. The theoretical maximum compressive strength of defect-free cement paste, estimated from the multi-scale model, wass as high as 3300 MPa [18].

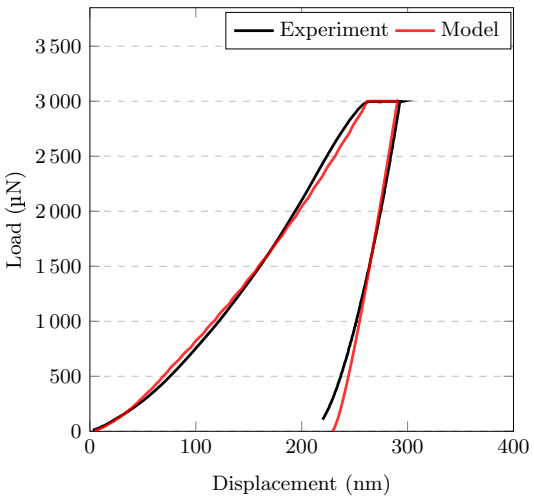

Figure 6: Typical experimental load-displacement curve (load level $3000\,\mu N$) measured on cement paste and the corresponding response calculated using the FE visco-elasto-plastic model.

Comparing these results and estimates with the least favorable conditions at a maximum force of $3000\,\mu N$, the calculated Von Mises stress of 958 MPa in the FE model reaches 61.4% of the average compressive strength of C–S–H found on micro-pillars, 17.1%–46.1% of the strength estimate using micro-beam bending, and 29.0% using the estimate from the multiscale model. These values generally fall bellow or within the standard range of 40–60% of the compressive strength [7], with a higher value found in comparison with the micro-pillar

testing. However, authors of the experiments reported a strong size effect depending on the diameter of the pillar [19]. The above comparisons further suggest that nanoindentation creep compliance falls within the linear creep regime.

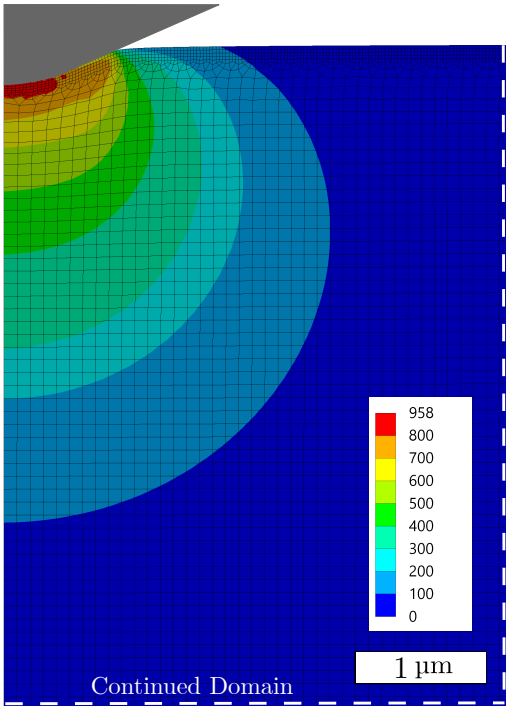

Figure 7: Distribution of Von Mises stress under the tip at the end of the holding period (load level 3000 µN) during nanoindentation of cement paste.

4 CONCLUSIONS

In this study, we aimed to demonstrate that the short-term creep compliance of C-S-H in cement paste, measured using nanoindentation with a Berkovich tip, falls within the linear creep regime. Our results show that the measured creep compliance is not dependent on the maximum vertical force of the tested interval, as evidenced by both the Kelvin chain and logarithmic models. Each of the models provided very similar predictions for creep compliance functions, with nearly identical viscoelastic constants for a variety of loads. The deviations between the individual compliance functions on cement sample were primarily attributed to its heterogeneity. The methodology and the conclusions were further validated by experiments on a homogeneous PMMA sample, where both models yielded identical creep compliance on a similar range of contact depths as for C-S-H.

When comparing the two used visco-elastic models with each other, different values could be observed. The logarithmic model generally provided approximately 2.7 times higher values of $J(t)$ at 40 s compared to the Kelvin chain model for both materials. The reason for this discrepancy is not clear and requires future analysis. In this context, the correction parameter of inelastic deformation, h_0, used with Kelvin chain model was found to increase linearly with the maximum force for both materials.

The maximum calculated Von Mises stress in the FE model (958 MPa for 3000 µN) aligns well with 40–60% compressive strength range derived from micro-beam testing, multi-scale models or average micro-pillar testing, where higher deviations are attributed to a significant size-effect. All these findings support the conclusion that nanoindentation creep compliance falls within the linear creep regime.

ACKNOWLEDGMENTS

This work was financially supported by the project of the Czech Science Foundation grant number 23-05435S.

REFERENCES

[1] Bažant, Z.P., and Wittmann, F.H. 1982. *Creep and Shrinkage in Concrete Structures*, John Wiley & Sons, Chichester (ISBN 0 471 10409 4).

[2] Vandamme, M., Tweedie, C.A., Constantinides, G., Ulm, F.-J., Van Vliet, K.J. 2012. Quantifying plasticity-independent creep compliance and relaxation of viscoelastoplastic materials under contact loading. *Journal of Materials Research* **27**:302–312.

[3] Oyen, M.L. 2007. Sensitivity of polymer nanoindentation creep measurements to experimental variables. *Acta Materialia* **55**:3633–3639.

[4] Vandamme, M., Ulm, F.-J. 2013. Nanoindentation investigation of creep properties of calcium silicate hydrates. *Cement and Concrete Research* **52**:38–52.

[5] Němeček, J., Trávníček, P., Keppert, M., Halodová, P., Rosnecký, V., Němeček, J. 2023. Nanomechanical analysis of Gamma-irradiated cement paste exposed to different humidities. *Materials Today Communications* **393**:131969.

[6] Sarris, E., Constantinides, G. 2013. Finite element modeling of nanoindentation on C–S–H: Effect of pile-up and contact friction. *Cement and Concrete Composites* **36**:78–84.

[7] Bažant, Z.P., and Jirásek, M. 2018. *Creep and hygrothermal effects in concrete structures*, Springer Dordrecht (ISBN 978-94-024-1136-2).

[8] Sorgner, M., Díaz Flores, R., Pichler, B., Pilgerstorfer, T., Moritz, B., Hellmich, C. 2025. Basic creep properties of hydrates in mature slag-based CEM II concretes: A micromechanical analysis. *Cement and Concrete Research* **189**:107735.

[9] Němeček, J., Lukeš, J., Němeček, J. 2020. High-speed mechanical mapping of blended cement pastes and its comparison with standard modes of nanoindentation. *Materials Today Communications* **23**:100806.

[10] Němeček, J., Němečková, J., and Němeček, J. 2024. Micro-scale creep of C-S-H quantified by nanoindentation and different evaluation methods. In *Concreep12 conference*; June 5–7, 2024, Delft University of Technology, Delft, The Netherlands.

[11] Oliver, W.C., Pharr, G.M. 1992. An improved technique for determining hardness and elastic modulus using load and displacement sensing indentation experiments. *Journal of Materials Research* **7**:1564–1583.

[12] Bažant, Z.P., Wu, S.T. 1973. Dirichlet Series Creep Function for Aging Concrete. *Journal of Engineering Mechanics* **99**:367–387.

[13] Němeček, J., Králík, V., Vondřejc, J. 2013. Micromechanical analysis of heterogeneous structural materials. *Cement and Concrete Composites* **36**:85–92.

[14] ANSYS Inc., *Ansys reference manual version 17.2*, 2019.

[15] Němeček, J., Králík, V., Šmilauer, V., Polívka, L., Jäger, A. 2016. Tensile strength of hydrated cement paste phases assessed by micro-bending tests and nanoindentation. *Cement and Concrete Composites* **73**:164–173.

[16] Hlobil, M., Šmilauer, V., Chanvillard, G. 2016. Micromechanical multiscale fracture model for compressive strength of blended cement pastes. *Cement and Concrete Research* **83**:188–202.

[17] Puttbach, C., Prinz, G.S., Murray, C.D. 2024. Strength and stiffness characterization of ultra-high performance concrete (UHPC) cement paste phases through in-situ micro-mechanical testing. *Cement and Concrete Composites* **149**:105520.

[18] Hlobil, M., Sotiriadis, K., Hlobilová, A. 2022. Scaling of strength in hardened cement pastes - Unveiling the role of microstructural defects and the susceptibility of C-S-H gel to physical/chemical degradation by multiscale modeling. *Cement and Concrete Research* **154**:106714.

[19] Shahrin, R., Bobko, C.P. 2019. Micropillar compression investigation of size effect on microscale strength and failure mechanism of Calcium-Silicate-Hydrates (C-S-H) in cement paste *Cement and Concrete Research* **125**:105863.